Atmos. Chem. Phys. Discuss., doi:10.5194/acp-2016-537, 2016
Manuscript under review for journal Atmos. Chem. Phys.
Published: 4 August 2016

Atmospheric Chemistry and Physics Discussions

Evolution of the eastward shift in the quasi-stationary minimum of the Antarctic total ozone column

Asen Grytsai[1], Gennadi Milinevsky[1], Andrew Klekociuk[2,3], Oleksandr Evtushevsky[1]

[1]Taras Shevchenko National University of Kyiv, 01601 Kyiv, Ukraine
[2]Antarctica and the Global System Program, Australian Antarctic Division, Kingston, Tasmania 7050, Australia
[3]Antarctic Climate and Ecosystems Cooperative Research Centre, Hobart, Tasmania 7000, Australia

Correspondence to: G. P. Milinevsky (genmilinevsky@gmail.com)

Abstract. The quasi-stationary pattern of the Antarctic total ozone has changed during the last four decades, demonstrating an eastward shift in the zonal ozone minimum. In this work, the association between the longitudinal shift of the zonal ozone minimum and changes in meteorological fields in austral spring (September–November) for 1979–2014 is analyzed. Regressive, correlative and anomaly composite analyses are applied to reanalysis data. Patterns of the Southern Annular Mode and quasi-stationary zonal waves 1 and 3 in the meteorological fields show relationships with interannual variability in the longitude of the zonal ozone minimum. On decadal time scales, consistent longitudinal shifts of the zonal ozone minimum and zonal wave 3 pattern in the middle troposphere temperature at the southern mid-latitudes are shown. As known, Antarctic ozone depletion in spring is strongly projected on the Southern Annular Mode in summer and impacts tropospheric climate. The results of this study suggest that changes in zonal ozone asymmetry accompanying the ozone depletion could be associated with regional climate changes in the Southern Hemisphere in spring.

Keywords: stratosphere, ozone hole, planetary wave, longitudinal shift, ERA-Interim climatology

1 Introduction

The distribution of total column ozone over Antarctica is significantly non-uniform during austral spring, i.e. in September–November (Wirth, 1993; Malanca et al., 2005; Grytsai et al., 2007a; Agosta and Canziani, 2010, 2011). This is particularly the case since the early 1980s due to the presence of ozone depletion associated with the ozone hole (Farman et al., 1985; Chubachi and Kajiwara, 1986; Solomon, 1999). The total ozone distribution predominantly characterizes the stratosphere layer where a sharp ozone maximum is usually observed at altitudes of 15-25 km (Solomon et al., 2005). Therefore, strong variations in the total ozone distribution are due mainly to stratospheric chemistry and dynamics (Wirth, 1993; Gabriel et al., 2011). The ozone hole is located

Atmos. Chem. Phys. Discuss., doi:10.5194/acp-2016-537, 2016
Manuscript under review for journal Atmos. Chem. Phys.
Published: 4 August 2016

Atmospheric Chemistry and Physics Discussions

inside polar stratospheric vortex, which is a cyclonic structure that impedes mixing between high-latitude and mid-latitude air masses (Brasseur et al., 1997). The polar vortex is under the influence of large-scale planetary waves, which disturb the vortex edge region (Wirth, 1993; Quintanar and Mechoso, 1995) and the vortex location relative to the pole (Waugh and Randel, 1999). The scale of the waves in the zonal direction is typically characterized by zonal wave number, which equals the ratio of the corresponding great circle circumference at a given latitude to the wave length (Hirota and Hirooka, 1984; Hio and Yoden, 2004). The stationary part of the wave structure in the Southern Hemisphere (SH) spring stratosphere is mainly determined by a planetary wave with zonal number 1 (Hartmann et al., 1984; Quintanar and Mechoso, 1995; Ialongo et al., 2012), i.e. wave-1. The role of planetary waves was especially important in the unusual SH stratospheric warming in 2002. Both wave-1 and wave-2 activity during austral winter and spring caused strong deceleration and warming of the stratospheric polar vortex, its anomalous splitting and ozone hole breakup in September 2002 (Nishii and Nakamura, 2004; Newman and Nash, 2005; Peters et al., 2007; Grassi et al., 2008; Peters and Vargin, 2015).

In spring, the ozone distribution in the Antarctic region is asymmetrical with a maximum in the Australian longitudinal sector and a minimum in the Atlantic longitudes (Grytsai et al., 2005; Agosta and Canziani, 2011). Previous studies have revealed the tendency of the Antarctic polar vortex to exhibit an eastward shift in orientation (Huth and Canziani, 2003), in the ozone minimum location (Grytsai et al., 2005; Malanca et al., 2005; Grytsai et al., 2007a, b; Agosta and Canziani, 2010, 2011; Grytsai, 2011; Hassler et al., 2011) and in the phase of wave-1 in stratospheric temperature (Lin et al., 2010). This eastward shift has been described as being possibly connected with a change in tropospheric stationary waves (Grytsai et al., 2007a), tropospheric jet structure (Hio and Hirota, 2002; Agosta and Canziani, 2011) and its strengthening (Wang et al., 2013), and stratospheric ozone and volcanic aerosol concentration (Lin et al., 2010). The quasi-stationary wave (QSW) activity increases typically in austral spring (Randel, 1988) and its enhancement leads to larger vortex asymmetry, a decrease in ozone hole area and net stratospheric ozone loss. It has been noted that the decreased (increased) asymmetry in the ozone distribution is associated with the eastward (westward) phase shift of the zonal minimum from both observations at the southern high latitudes (Grytsai et al., 2008; Agosta and Canziani, 2011) and climate model simulations for the northern high latitudes (Gabriel et al., 2007).

Recent studies have indicated that a stabilization of the spring ozone depletion over the southern high latitudes has occurred from the mid- or late 1990s (Grytsai, 2011; Salby et al., 2011; Kuttippurath et al., 2013; Dameris and Godin-Beekmann, 2014, Solomon et al., 2016). This stabilization relates to the total area of the ozone hole, minimum total ozone values, ozone mass deficit and duration of the ozone hole season. Chemistry-climate models have displayed a general minimum in Antarctic ozone during 2000–2005 (Siddaway et al., 2013) and slow ozone recovery in the 21st century (Dameris and Godin-Beekmann, 2014). This work is focused on the recent tendencies in the zonal asymmetry of the Antarctic total ozone in austral spring.

Atmos. Chem. Phys. Discuss., doi:10.5194/acp-2016-537, 2016
Manuscript under review for journal Atmos. Chem. Phys.
Published: 4 August 2016

Atmospheric Chemistry and Physics Discussions

2 Data and methods

In this study, gridded monthly-mean satellite measurements of the total ozone column (TOC) are used to estimate tendencies in the Antarctic quasi-stationary pattern. We restrict our analysis to the September to November (SON) period (austral spring) when the zonal asymmetry in total column ozone is most pronounced. We use measurements from the Total Ozone Mapping Spectrometer (TOMS) / Nimbus-7 (1979–1992), TOMS / Earth Probe (1996–2005) and Ozone Monitoring Instrument (OMI) aboard the Aura platform (2006–2015) which were obtained from the NASA Ozone & Air Quality website http://ozoneaq.gsfc.nasa.gov/. A gap between Nimbus-7 and Earth Probe observations in 1993–1995 was filled in by Multi Sensor Reanalysis (MSR) data (http://www.temis.nl; van der A et al., 2010).

The original data were obtained with latitude and longitude resolutions of 1° and 1.25°, respectively. We averaged the data over each SON interval to suppress the effects of long-period travelling planetary waves (Grytsai et al., 2007a), and selected zonal values from 50°S to 80°S at 5° latitude intervals; the centres of our selected latitude bins are 50.5°S, 55.5°S, … 80.5°S. The zonal asymmetry in the TOC distribution over this latitude range is illustrated by Fig. 1. As seen from Fig. 1a, the TOC field in the austral spring has the two zonally asymmetric components noted in Section 1. First, the stratospheric polar vortex and ozone hole (blue) are displaced relative to the South pole and, second, the TOC field has the clear zonal maximum (red) at the subantarctic and middle latitudes. As a result, longitudinal TOC distributions demonstrate wave-1 structure in the SH midlatitude and polar zone. Figure 1b shows long-term changes in the zonal TOC asymmetry at 65°S (white circle in Fig. 1a) during 1979–2014. In 2000s (blue curves in Fig. 1b), when ozone loss culminated, zonal TOC minimum is by about 100 DU lower, than in the pre-ozone hole years (red curves) and is notably displaced to the east. This illustrates a general tendency for the zonal TOC minimum to be located further eastward with decreasing minimum level noted previously (Grytsai et al., 2005; Lin et al., 2010; Agosta and Canziani, 2011; Hassler et al., 2011). For the quantitative analysis, the longitudes of the zonal TOC maximum and minimum were determined using a 50-degree window in longitude to separate out the large-scale parts of the disturbances.

In this work, long-term tendencies were obtained from polynomial approximation calculated with a least-squares method. The calculations were carried out with a following scheme (see, e.g. Krishnan, 2006). Let us consider n pairs of values (x_i, y_i). The purpose is to find a polynomial fit of degree k to minimize

$$f(x_i, y_i) = \sum_{i=1}^{n} (P_k(x_i) - y_i)^2$$

where

$$P_k(x_i) = \sum_{m=0}^{k} a_m x_i^m$$

is a polynomial of k-th power with unknown coefficients a_j. The minimization condition for the function f is written as

Atmos. Chem. Phys. Discuss., doi:10.5194/acp-2016-537, 2016
Manuscript under review for journal Atmos. Chem. Phys.
Published: 4 August 2016

Atmospheric Chemistry and Physics Discussions

$$\frac{\partial f}{\partial a_j} = 0\,,$$

which includes a system from $k + 1$ equations for different j. In solving the system we obtain each coefficient as the ratio of the two determinants:

$$a_m = \frac{\begin{vmatrix} n & \sum_{i=1}^{n} x_i & \dots & \sum_{i=1}^{n} x_i^{m-1} & \sum_{i=1}^{n} y_i & \dots & \sum_{i=1}^{n} x_i^{k} \\ \dots & \dots & \dots & \dots & \dots & \dots & \dots \\ \sum_{i=1}^{n} x_i^{k} & \sum_{i=1}^{n} x_i^{k+1} & \dots & \sum_{i=1}^{n} x_i^{k+m-1} & \sum_{i=1}^{n} x_i^{k} y_i & \dots & \sum_{i=1}^{n} x_i^{2k} \end{vmatrix}}{\begin{vmatrix} n & \sum_{i=1}^{n} x_i & \dots & \sum_{i=1}^{n} x_i^{m-1} & \sum_{i=1}^{n} x_i^{m} & \dots & \sum_{i=1}^{n} x_i^{k} \\ \dots & \dots & \dots & \dots & \dots & \dots & \dots \\ \sum_{i=1}^{n} x_i^{k} & \sum_{i=1}^{n} x_i^{k+1} & \dots & \sum_{i=1}^{n} x_i^{k+m-1} & \sum_{i=1}^{n} x_i^{k+m} & \dots & \sum_{i=1}^{n} x_i^{2k} \end{vmatrix}}$$

Beside the whole quasi-stationary pattern, separate spectral Fourier harmonics were also evaluated. Their parameters were calculated from the same quasi-stationary averaged distributions. The amplitude A_m and phase λ_m of the harmonics were obtained as in Varotsos et al. (2008):

$$A_m = \frac{1}{\pi}\left[\left(\int_{-\pi}^{\pi} f\ \lambda\ \cos m\lambda d\lambda\right)^2 + \left(\int_{-\pi}^{\pi} f\ \lambda\ \sin m\lambda d\lambda\right)^2\right]^{1/2}$$

$$\lambda_m = \frac{1}{m}\arccos\left(\frac{1}{\pi A_m}\int_{-\pi}^{\pi} f\ \lambda\ \cos m\lambda d\lambda\right)\cdot \mathrm{sgn}\left(\int_{-\pi}^{\pi} f\ \lambda\ \sin m\lambda d\lambda\right).$$

Here m is number of a zonal harmonics (e.g. m = 1 for wave-1) and $f(\lambda)$ corresponds to the zonal ozone distribution. Respective to this definition, we use 'phase' to refer only to the longitude of a wave maximum in the ozone distribution.

In addition to the TOC data, we use gridded atmospheric variables from the European Centre for Medium-Range Weather Forecasts (ECMWF) reanalysis ERA-Interim (Dee et al., 2011; http://www.ecmwf.int/en/research/climate-reanalysis/era-interim) and NCEP–NCAR reanalysis 1 (Kalnay et al., 1996; http://www.esrl.noaa.gov/psd/).

3 Results

3.1 Longitudinal changes in the QSW structure

First, we compare the long-term changes in total ozone (Fig. 2a) and the longitudinal position of the quasi-stationary ozone minimum (Fig. 2b) at 65°S latitude, which is located in the edge region of the ozone hole and polar stratospheric vortex (Roscoe et al., 2012) and where the largest QSW amplitude is observed (Grytsai et al., 2007a; Ialongo et al., 2012).

The results of calculations with polynomial fitting of degree k = 3 (Section 2) are shown by thick curves. In the early 2000s, the decadal tendencies changed sign in both ozone (from decreasing levels to increasing levels, Fig. 2a) and in ozone minimum longitudes (from eastward shift to

Atmos. Chem. Phys. Discuss., doi:10.5194/acp-2016-537, 2016
Manuscript under review for journal Atmos. Chem. Phys.
Published: 4 August 2016

Atmospheric Chemistry and Physics Discussions

westward shift, Fig. 2b). Comparison of polynomials from k = 2 to k = 6 gives similar opposite tendencies before and after the early 2000s (not shown). The quasi-stationary maximum in total ozone at 65°S shows a relatively small decadal shift in longitude (Fig. 2c, thick curve).

The observed consistency in cessation of the TOC decrease and eastward shift in the zonal TOC minimum suggest that these are coupled phenomena. The eastward shift in the QSW structure over Antarctica was described earlier (Huth and Canziani, 2003; Grytsai et al., 2005, 2007a; Malanca et al., 2005; Agosta and Canziani, 2010, 2011; Lin et al., 2010; Grytsai, 2011; Hassler et al., 2011). The eastward shift speeds of about 15–20°/decade are consistent among various studies (Grytsai et al., 2007a; Lin et al., 2010; Hassler et al., 2011). For the period 1979–2000, the time series in Fig. 2b gives a linear trend of 14.4±12.5°/decade, significant at the 95% level. The westward shift between the early 2000s and early 2010s in Fig. 2b is statistically insignificant and a longer data set is necessary to reliably establish this tendency. Note that Fig. 2b shows large longitude variations during the most recent years. Interannual changes in the 2000s and early 2010s covered a wider longitudinal range than in the previous decades. For example, the position of the quasi-stationary minimum was near its extreme western values in 2011 and 2013, whereas it reached the farthest eastern longitude in 2010.

Long-term tendencies in the QSW minimum/maximum longitudes at the seven latitudes between 50°S and 80°S are illustrated in Fig. 3. The TOC extreme longitudes for 1979, 2002 and 2015 are obtained from cubic polynomial as shown by closed circles in Fig. 2b. Significant eastward shift of the QSW minimum from 1979 (solid blue curve) to the early 2000s (dotted blue curve for 2002) by 30–60 degrees of longitude is seen. The curve for 2015 in the region of the zonal TOC minimum (black dotted curve in Fig. 3) is located between the curves for 1979 and 2002 and was shifted westward over the whole zone 50–80°S, which was towards the opposite extreme compared with most years of the preceding decade. Changes of the QSW maximum longitudinal position are not regular (Grytsai et al., 2007a) and the largest eastward shifts are seen only at 55°S and 60°S, however, they are not statistically significant due to strong interannual variability (Fig. 2c). Relative stability of the zonal maximum suggests that higher zonal wave numbers, QSW2 and QSW3, could be present in the QSW structure, in addition to the dominant QSW1 (Grytsai et al., 2007a; Agosta and Canziani, 2011).

The two curves in Fig. 4 illustrate the similarity in the interannual variations and decadal changes of the QSW minimum longitudes and ozone mass deficit in Antarctic spring. The correlation between the two variables is positive (r = 0.49–0.57 for the seven latitude circles between 50°S and 80°S with maximum at 60°S), hence, an eastward shift of the QSW minimum in the ozone distribution corresponds to a greater ozone mass deficit (larger ozone loss).

Simultaneous negative deviations are observed in the years of large (1988) and extreme (2002) stratospheric warmings (vertical lines), when relatively small ozone mass deficits (high total ozone levels) correspond to the westward shift of the QSW minimum position. Note that this correspondence is not observed in some recent years; the Antarctic spring in 2010 is characterized by eastern longitude of the QSW minimum at low ozone mass deficit, and the relationship for 2011 is opposite.

Atmos. Chem. Phys. Discuss., doi:10.5194/acp-2016-537, 2016
Manuscript under review for journal Atmos. Chem. Phys.
Published: 4 August 2016

Atmospheric Chemistry and Physics Discussions

Eeastward shift in the TOC zonal minimum longitude in the Antarctic region is occurred during 1980s–1990s. This decadal tendency appears to have stopped in the early 2000s and became of possibly reverse sign later in the 2000s and 2010s. Generally, the behavior of the zonal TOC minimum follows the decadal change in the severity of the ozone hole due to international controls on ozone depleting substances (Salby et al., 2011), with increasing depletion of the Antarctic ozone in 1980s and 1990s, leveling off in the SH polar TOC levels and the possible start of ozone hole recovery in 2000s–2010s. Significant decadal changes in the SH polar ozone are coupled with the stratospheric thermal regime, and, because of the zonal asymmetry in the ozone heating, they may impact planetary wave propagation and regional climate change in both the troposphere and the stratosphere (Crook et al., 2008; Gillet et al., 2009; Waugh et al., 2009; Albers and Nathan, 2012). Possible coupling between changes in the QSW structure in Antarctic total column ozone and in atmospheric variables is analyzed below.

3.2 Relationships between the QSW minimum longitude and meteorological parameters

To determine the most reliable mean tendencies, we have created a time series for the QSW minimum (QSW_{min}) longitudes averaged between 55°S and 70°S (four latitude circles in Fig. 3); this is shown in Fig. 5. Bars in Fig. 5 indicate standard deviations for each year and they are generally quite small.

We next consider the regression between the time series of Fig. 5 and climatological anomalies of deseasonalised meteorological variables using ERA-Interim data. The SON mean ERA-Interim climatological anomalies were obtained removing long-term montly means for September, October and November in each grid box of 10°×10° (latitude × longitude) size. Global distribution of the regression coefficients (RC) between the QSW_{min} longitude and ERA-Interim climatological anomalies of surface pressure (SP) and 2 metre air temperature (T-2m), for SON 1979–2014 is presented in Figs 6a and 6b, respectively. Dots with numbers from 1 to 5 in Fig. 6a are placed at each grid box centre, where the linear correlation coefficient is significant at the 95% confidence limit based on Student's *t*-test (boxes with significant correlations are also diagonally hatched) and where the fraction of variance explained (values in %) is ≥ 25% (see text below).

The RC distribution as in Fig. 6a and 6b, but for RC between the QSW_{min} longitude and ERA-Interim 200-hPa climatological anomalies of zonal wind speed (U200) and vertical pressure wind speed (W200) are shown in Fig. 6c and 6d, respectively. The pressure level of 200 hPa corresponds to the upper troposphere in the tropics and lower stratosphere in the SH extratropics and is usually used to analyze the interaction between the tropics and extratropics (e.g. Mo and Higgins, 1998). The RC distribution for sea surface temperature (SST) is similar for that for T-2m (Fig. 6b) and the RC distribution for meridional wind V200 is similar to that for W200 (Fig. 6d), and are not shown here.

The RC distribution in Fig. 6a shows nearly an annular pattern that is similar to a classic Southern Annular Mode (SAM) pattern in SH climate variability, with pressure or geopotential height anomalies of opposite sign in the middle and high latitudes (Thompson and Wallace, 2000).

Atmos. Chem. Phys. Discuss., doi:10.5194/acp-2016-537, 2016
Manuscript under review for journal Atmos. Chem. Phys.
Published: 4 August 2016

Atmospheric Chemistry and Physics Discussions

Negative (positive) regression coefficients in the high (middle) SH latitudes indicate that the QSW_{min} eastward shift is associated with decreased (increased) surface pressure, i.e. with the SAM deviation to positive polarity.

A positive polarity of the annular mode is accompanied by strengthening of the subpolar westerlies in the SH troposphere and stratosphere and cooling of polar cap regions (Thompson and Wallace, 2000). The RC maximum around 60°S in Fig. 6c and the RC minimum over the Antarctic continent (poleward of 60°S) in Fig. 6b display similar tendencies in the relationships between the QSW_{min} eastward shift and increase of U200 and decrease of T-2m, respectively.

Zonally asymmetric components of the SH circulation, which are most marked in the austral winter and spring (Mo and Higgins, 1998; Fogt et al., 2012a), are also presented in Fig. 6. Three positive RC anomalies in the SH midlatitudes (grid boxes 1, 2 and 3 in Fig. 6a) demonstrate the presence of a QSW wave-3 (QSW3) structure. The highest negative RC anomaly between grid boxes 2 and 3 is spatially close to the subpolar negative anomaly at grid box 4 and is possibly combined effect of QSW wave-1 (QSW1) and QSW3 (Mo and Higgins, 1998). A significant negative RC anomaly near West Antarctica (grid box 4 in Fig. 6a with an explained variance of 35%) is spatially coincident with the 'pole of variability' in the Amundsen–Bellingshausen Sea Low (ABSL) region (Fogt et al. 2012b and references therein; Turner et al., 2013; Raphael et al., 2016). The midlatitude QSW3 patterns extended to sub-Antarctic latitudes are seen also in the RC distribution for T-2m and W200 (Fig. 6b and 6d, respectively).

The presence of the QSW3 structure in Fig. 6b introduces regional anomalies in the surface temperature distribution. The patterns suggest that when the QSW_{min} moves to the east, surface temperatures are warmer in the Antarctic Peninsula–Weddell Sea region and in the south–west area of Indian Ocean, and cold anomalies appear in the South Pacific and south-east Australia.

Zonal asymmetry in the SH troposphere circulation is closely coupled with the Pacific–South American (PSA) mode (Mo and Higgins, 1998). However, the PSA pattern in the RC distribution in Fig. 6 is of insignificant intensity, whereas pronounced meridional wave trains are seen in Indian–Australian sector and Atlantic–South American sector (U200 in Fig. 6c).

In general, Fig. 6 shows that interannual variations of the SON QSW_{min} longitude during 1979–2014 are mainly associated with the zonally symmetric annular mode and zonally asymmetric QSW structures. To contrast the SH circulation changes connected to the QSW_{min} eastward shift, Fig. 7 presents the results of more differentiated analysis. The ERA-Interim anomaly composites of the surface meteorological variables relative to climatology 1979–2014 were created separately for the eastern and western QSW_{min} longitudes. Anomaly composites for the lower 20^{th} percentile of the QSW_{min} longitudes (<–60° longitude, 8 westernmost locations outlined by dashed rectangle in Fig. 5a) are presented in Fig. 7a–7c. Anomaly composites for the higher 80^{th} percentile (>–3.8° longitude, 8 easternmost locations outlined by solid rectangle in Fig. 5a) are presented in Fig. 7d–7f. The years for the westernmost longitudes are 1979, 1980, 1981, 1988, 1990, 2002, 2011 and 2013 (left column of Fig. 7) and the years for the easternmost longitudes are 1985, 1992, 1998, 2001, 2003, 2006, 2008 and 2010 (right column of Fig. 7).

Atmos. Chem. Phys. Discuss., doi:10.5194/acp-2016-537, 2016
Manuscript under review for journal Atmos. Chem. Phys.
Published: 4 August 2016

Atmospheric Chemistry and Physics Discussions

It is seen from Fig. 7 that transition from the westernmost longitudes (left column) to the easternmost longitudes (right column) is associated with sign reversal of the anomalies. The western (eastern) longitudes correspond to negative (positive) zonal wind anomaly around 60°S in Fig. 7a (7d) and positive (negative) surface pressure poleward of 60°S in Fig. 7b (7e). Opposite anomaly combinations appear in the SH middle latitudes. These changes are consistent with the regression maps in Fig. 6a and 6c, where eastward phase shift indicates similar relationships with U200 (Fig. 6c) and SP (Fig. 6a).

Note that the SP anomaly composites show the QSW3-like structure in the SH midlatitudes, which is more intense and shifted to the east in a case of the easternmost QSW_{min} longitudes than in a case of the westernmost longitudes (Fig. 7e and 7b, respectively). This is clear evidence of the coupling between eastward shifts in the stratospheric QSW structure of the SH polar region (represented by the QSW_{min} longitude) and tropospheric QSW3 structure in the SH midlatitudes. Consistent shifts in the QSW patterns in the troposphere and stratosphere during the last decades seem to be a manifestation of possible feedbacks between the zonally asymmetric ozone loss and QSW propagation from the troposphere to the stratosphere in austral spring (Crook et al., 2008; Albers and Nathan, 2012).

The SST anomaly composites demonstrate a relationship of the extreme QSW_{min} longitudes with different tropical regions: western (eastern) longitudes in Fig. 7c (7f) are observed for the negative SST anomalies in the eastern (central) tropical Pacific. The negative tropical SST anomalies are not as extended and intense as anomalies in the SH extratropics for other variables in Fig. 6 and Fig. 7.

It should be noted that difference between the two regions of the tropical Pacific in their coupling with the QSW structure in the SH stratosphere was noted by Lin et al. (2012). By Lin et al. (2012), westward QSW phase shift is seen for negative SST anomalies (La Nina events) in the eastern Pacific and eastward shift is seen for warm SST anomalies in the central Pacific. The result of Fig. 7c shows a similar association between the westernmost QSW_{min} longitudes and negative SST anomaly in the eastern Pacific (La Nina type anomaly). However, the easternmost longitudes in Fig. 7f show also a negative anomaly in the central Pacific, as distinct from a positive one (Lin et al., 2012).

On the other hand, the easternmost longitudes in Fig. 7f demonstrate positive SST anomalies in the western tropical Pacific and in Atlantic, similarly to the same anomaly locations in T-2m in Fig. 6b. Such positive anomaly distributions resemble the pattern of the anomalous SST trend calculated with zonal mean trend removed (Schneider et al., 2015, their Fig. 2f). Additionally, the significant positive RC anomaly for T-2m in the Antarctic Peninsula/Weddell Sea region (35% of variance explained, Fig. 6b) may indicate a contribution of the Atlantic SST anomalies to both warming in this region (e.g. Li et al., 2014) and the QSW structure in total ozone.

Compared with other surface variables in Fig. 7, which show clear patterns of SAM (Fig. 7a and 7d) and QSW3 (Fig. 7b and 7e), the SST anomalies in Fig. 7c and 7f look less associated with the QSW_{min} longitude. Remember also the absence of the significant PSA pattern in U200 (Fig. 6c), which is typically generated by the SST anomalies in the tropical Pacific (Mo and Higgins, 1998).

Atmos. Chem. Phys. Discuss., doi:10.5194/acp-2016-537, 2016
Manuscript under review for journal Atmos. Chem. Phys.
Published: 4 August 2016

Atmospheric Chemistry and Physics Discussions

Close connection between the QSW_{min} longitudes and the SAM/QSW3 patterns (Fig. 6 and Fig. 7) is further confirmed by Fig. 8. Regression of the QSW_{min} longitudes against the SP anomalies at grid box 1 (42.5°S, 65.0°E; Fig. 6a), a mid-latitude element of QSW3, is shown in Fig. 8a. A close similarity can be seen in variations of the SP anomalies in grid box 1 and the QSW_{min} longitudes averaged over 55–70°S: the square of the linear correlation coefficient is $r^2 = 0.57$.

In Fig. 8b, timeseries of the QSW_{min} longitude and the standardized SAM index (Marshall, 2003; https://climatedataguide.ucar.edu/climate-data/marshall-southern-annular-mode-sam-index-station-based) are shown. The square of the linear correlation coefficient between the two timeseries $r^2 = 0.35$. Therefore, approximately 57% and 35% of the QSW_{min} longitude variance (both significant at the 95% confidence limit) can be explained by the surface pressure anomalies described by regional (grid box 1, QSW3 pattern) and hemispheric-scale (SAM) indices, respectively. This indicates that a significant interaction takes place between the identified anomalies in the tropospheric circulation and the quasi-stationary wave structure in the SH stratosphere.

As noted from Fig. 6c, the regression coefficient distribution for U200 shows meridional wave trains in the Indian and Atlantic sectors. To contrast the result of Fig. 6c, anomaly composites as in Fig. 7 but for 200 hPa are presented in Fig. 9. Similarly to Fig. 7, transition from the westernmost QSW_{min} longitudes to easternmost ones (left and right columns, respectively) is accompanied by the anomaly sign reversal. The U200 anomaly composites in Fig. 9b and 9f show likely meridional wave train patterns over the three ocean basins, however, without clear eastward propagation, and it is difficult to determine the wave train sources.

It is important to note the eastward shift of the anomalies between the westernmost and easternmost QSW_{min} longitudes. It can be seen comparing, for example, the QSW1 patterns in T200 at the middle–high SH latitudes (Fig. 9a and 9e) and the QSW3 patterns in W200 at the middle–sub-Antarctic latitudes (Fig. 9c and 9g). Note also more intense anomalies for the easternmost QSW_{min} longitudes in Fig. 9 (right column), which demonstrate lower temperature over large part of the middle–high SH latitudes (T200, Fig. 9e), stronger sub-Antarctic zonal circulation in the lower stratosphere (U200, Fig. 9f) and enhancement of the QSW3 patterns in vertical velocities (W200, Fig. 9g) and eddy heat flux (V′T′200, Fig. 9h). Since the easternmost longitudes characterize mainly 1990s and 2000s (as outlined by solid rectangle in Fig. 5), the right column in Fig. 9 could indicate that the two decades of the strongest ozone loss were favorable for the closest interaction between the SAM/QSW3-related anomalies and the QSW structure in total ozone.

In connection between the changes in the QSW structure in total ozone and atmospheric parameters, the clear eastward shift in the QSW3 patterns (Fig. 7b and 7e and Fig. 9c and 9g) is of particular interest. An alternative analysis tool and data are used in further consideration. The linear correlation between timeseries of the QSW_{min} longitude at 65°S and the NCEP–NCAR reanalysis air temperature was evaluated. As the QSW3 structure is concentrated in the mid- and sub-Antarctic latitudes (Figs. 6, 7 and 9), the correlation for air temperature averaged over the zone 40–60°S was calculated. In Fig. 10, the results in the longitude–height cross-section (http://www.esrl.noaa.gov/psd/data/correlation/) for the 36-year period 1979–2014 are presented.

Atmos. Chem. Phys. Discuss., doi:10.5194/acp-2016-537, 2016
Manuscript under review for journal Atmos. Chem. Phys.
Published: 4 August 2016

Atmospheric Chemistry and Physics Discussions

The sample sizes in this case mean that correlation r = 0.27 is significant at the 95% confidence limit (black and white contours in Fig. 10 for the positive and negative correlations, respectively).

A clear separation between the QSW1 pattern above the tropopause (peak values of r = ±0.7; climatological thermal tropopause from the NCEP–NCAR reanalysis is shown by black curve) and the QSW3 pattern below the tropopause ($r_{max} \approx 0.5$) is seen. An important feature of the QSW3 pattern is its altitudinal location: the three correlation maxima are located predominantly in the middle troposphere and their peak values are at about 500 hPa (Fig. 10). The correlation is significantly lower at 1000 hPa which could explain relatively weak SST anomalies in the SH midlatitudes in Fig. 7c and 7f. Therefore, the mid-tropospheric pressure level of 500 hPa was chosen for search of possible decadal changes in the correlations between the anomalies in air temperature and in the QSW_{min} longitudes. In Fig. 11, correlation coefficient distributions in a sequence of the five 14-year intervals with the 5–6 year steps are shown. The sample size N = 14 and calculated lag-one autocorrelations give significance level of 95% for the correlation coefficient r = 0.51.

It is seen that the significant positive correlation peaks (black contours in Fig. 11) shift eastward between 1979–1992 and 1990–2003 by 30–60 degrees (thick lines in Fig. 11a–11c). Later, they remain in average at the easternmost longitudes in 1995–2008 and 2001–2014 (Fig. 11d and 11e, respectively). The QSW3 peak near 180°E exhibits a shift in opposite direction in the last time interval (Fig. 11e).

A significant negative anomaly of the correlation coefficient (r < –0.5, white contours) in the South Pacific extending to polar latitudes into the Amundsen Sea low region is longitudinally steady (white dashed line). As noted above concerning similar anomaly location in the RC distributions in Fig. 6a and 6b, this could be combined effect of QSW1 and QSW3. Here, meteorological variables in troposphere are correlated with the QSW_{min} longitude in total ozone in their interannual variation, but do not show consistent decadal changes in spatial pattern. Note that annual cycle in the decadal shift of the ABSL longitude could contribute to distinction in zonal shift of the correlation anomalies at the middle and high SH latitudes in Fig. 11. The ABSL shifted westward in average by –5°/decade in September–November 1979–2008 (Turner et al., 2013, their Fig. 13) that could partly compensate eastward shift observed in the correlation maxima of the adjoining midlatitudinal zone (Fig. 11).

It can be summarized that common decadal tendencies in total ozone (Fig. 2a), QSW minimum in the total ozone field (Fig. 2b), QSW1 pattern in the lower stratosphere (Fig. 9a and 9e) and QSW3 pattern in the troposphere (Fig. 7b and 7e and Fig. 11) and lower stratosphere (Fig. 9c and 9g) exist. Note also that, because Figs. 6–11 present the relationships on a seasonal time scale, the statistically significant results seem to reveal new features of the troposphere–stratosphere interaction in Antarctic spring (September–November). The SAM- and QSW1/QSW3-like patterns in the SH circulation associated with variability in the QSW minimum longitude in total ozone are dominating.

4 Discussion and conclusions

Atmos. Chem. Phys. Discuss., doi:10.5194/acp-2016-537, 2016
Manuscript under review for journal Atmos. Chem. Phys.
Published: 4 August 2016

Atmospheric Chemistry and Physics Discussions

The evolution of zonal asymmetry in Antarctic total ozone during 1979–2014 with respect to the changes in the meteorological variables in the troposphere and lower stratosphere has been analyzed. Regressive, correlative and anomaly composite analyses show that longitudinal shift of the quasi-stationary zonal TOC minimum has a close relationship with changes in the SAM and QSW patterns in the SH troposphere and lower stratosphere. The main results are:

1) In interannual variations, the longitude of the QSW minimum in total ozone is in close association with the SAM index and the QSW3 pattern in the meteorological variables. Particularly, easternmost (westernmost) longitudes of the QSW minimum correspond to positive (negative) SAM polarity (Fig. 8b).

2) The shift of the QSW minimum in total ozone to the easternmost longitudes is accompanied by the midlatitude QSW3 enhancement, as seen from the anomaly composites for SP (Fig. 7e), and vertical velocity (W200 in Fig. 9g) and eddy heat flux (V′T′200 in Fig. 9h) in the upper troposphere – lower stratosphere region. Simultaneously, the eastward shift of both the QSW3 pattern in SP (Fig. 7e) and in W200 (Fig. 9g) and QSW1 pattern in T200 (Fig. 9e) occur.

3) On the decadal time scale, a relationship between the longitudinal shifts of the QSW minimum in total ozone and the QSW3 pattern in the mid-tropospheric temperature (Fig. 11) has been demonstrated.

The results, thus, reveal indications of the connection between changes in zonal asymmetry in Antarctic total ozone and changes in zonally symmetric (SAM) and zonally asymmetric (QSW1 and QSW3) patterns in the SH circulation. These results are, in general, in agreement with known evidence of coupling between Anarctic ozone, SAM and SH QSW structure (Thompson and Wallace, 2000; Malanca et al., 2005; Wang et al., 2013).

As is known, positive SAM polarity is associated with the enhanced westerlies around Antarctica and decreased surface pressure and air temperature in the polar region (Thompson and Wallace, 2000). The eastward shift of the QSW minimum in total ozone is accompanied by similar indications of the positive SAM polarity: strengthening of zonal wind around Antarctica (U-10m in Fig. 7d and U200 in Fig. 9f), surface pressure decrease (SP in Fig. 7e) and air temperature decrease (T-200 in Fig. 9e and T500 in Fig. 11) in the SH high latitudes. A large part of the QSW_{min} longitude variance can be explained by the SAM-index variance (35%, Fig. 8b).

Our results do not give information on the direction of the 'QSW_{min}–SAM' coupling: tropospheric circulation disturbances can influence the evolution of the stratospheric polar vortex and, in turn, stratospheric processes can induce a tropospheric response that projects on the annular mode (Thompson ans Wallace, 2000). It is known that the Antarctic ozone losses in spring impact the SAM-related tropospheric circulation predominantly in summer (Thompson et al., 2011; Schneider et al., 2015) and the spring SAM index shows near-zero decadal trend (Fogt et al., 2009; Arblaster and Gillett, 2014). In addition, in our relationships for zonal wind (Fig. 7a and 7d and Fig. 9b and 9f), it is difficult to reveal evidence of the poleward shift of the westerly jets observed usually in the positive SAM polarity (Thompson and Wallace, 2000). This is because of strong disturbance of zonal anomaly orientation by the midlatitude QSW3 structure. So, on decadal time scale, influence

Atmos. Chem. Phys. Discuss., doi:10.5194/acp-2016-537, 2016
Manuscript under review for journal Atmos. Chem. Phys.
Published: 4 August 2016

Atmospheric Chemistry and Physics Discussions

of the ozone change accompanied by the QSW_{min} longitude change (Fig. 2a and 2b, respectively) on the spring SAM pattern looks unlikely.

Nevertheless, such feedback possibility can not be fully excluded, at least on interannual time scales. As shown by Son et al. (2013), stratospheric ozone concentration in September is strongly correlated with the SAM index in October with r = –0.7. The mechanism of this time-lagged downward coupling remains to be determined. Agosta and Canziani (2011) have shown that there are significant interactions/coupling between the ozone layer, the troposphere, and the stratosphere during the austral spring, which can be traced by the phase changes in TOC and QSW1 in the stratosphere. Such changes and troposphere–stratosphere interactions, by Agosta and Canziani (2011), are linked to both the upward and downward propagation of quasi-stationary wave anomalies.

Note that the basic parameter analyzed in this work, the QSW_{min} longitude, characterizes change in the zonal asymmetry of the Antarctic total ozone field. Zonal asymmetry in ozone loss can influence the QSW propagation from the troposphere to the stratosphere in austral spring (Crook et al., 2008; Albers and Nathan, 2012) favoring feedbacks between the zonally asymmetric anomalies in ozone heating of the lower stratosphere and tropospheric anomalies. Our analysis is based on seasonal means (September–November) and such feedback processes in troposphere–stratosphere interaction are potentially feasible on this timescale.

Thus, the appearance of the SAM-like patterns in our relationships (Fig. 6, Fig. 7 and Fig. 9) can be interpreted in two ways that are influenced by interannual variability: first, the strength and pattern of the circulation in the spring SH troposphere can conceivably play a significant role in determining the location of the QSW structure in the stratosphere, and, second, the QSW structure in the stratosphere can potentially provide a downward influence on the tropospheric circulation.

Unlike the SAM pattern, the atmospheric QSW3 pattern in the midlatitude troposphere demonstrates long-term changes (Fig. 11) consistent with both the ozone loss tendency (Fig. 2a and Fig 4, black curve) and the QSW_{min} longitude shift (Fig. 2b). Positive correlations of up to r = 0.7–0.8 and the longitudinal shift of the three correlation maxima in Fig. 11 are evidence of significant coupling between QSW_{min} and QSW3 on both interannual and decadal time scales. QSW3, although smaller than QSW1, is a dominant feature of the SH midlatitude circulation on daily, seasonal and interannual timescales (Raphael, 2004, and references therein). The QSW3 ridges determined from the 500-hPa geopotential height anomalies over the period 1958–2001 by Raphael (2004), are located climatologically over southern South America, the southern Indian Ocean and southwest of New Zealand. Those ridge locations correspond to the correlation maxima in Fig. 11a and 11b for the periods 1979–1992 and 1984–1997, respectively, which cover the last two decades of the time interval in Raphael (2004). The largest eastward shift of the QSW3 pattern occurred between the 1980s and 1990s (Fig. 11a and 11c, respectively). The central ridge that is located on average near 180° E (Fig. 10) drifted from the southwest of New Zealand in the 1980s (as in Raphael (2004) and shown in Fig. 11a) to southeast of New Zealand by the early 2000s (Fig 11d), covering over about 60° of longitude. Apparent in the longitude sector of this ridge in the 1990s and 2000s has been a cooling of the tropical central Pacific that has been linked to wind-driven vertical

circulation changes in the Pacific Ocean (England et al., 2014); this process is also associated with the spin-up of the subtropical gyres and associated surface ocean warming (see Fig. 2 of England et al. (2014)) in the region of the ridge. In the 2000s and 2010s, as seen from Fig. 11c–11e, the ridge locations showed less drift. In particular, Figure 11e indicates that the central ridge has drifted west back towards New Zealand.

Overall, the shifts in the QSW3 centers in Fig. 11 show a temporal evolution that is qualitatively similar to decadal changes in both ozone depletion (Fig. 2a and Fig. 4, black curve) and the shift of QSW_{min} in total ozone (Fig. 2b). This similarity suggests that decadal-scale changes in the location of QSW structures in the troposphere and stratosphere appear to influence or be influenced by the locations of zonal anomalies in tropospheric temperature and stratospheric ozone. Chemistry-climate models predict that the Antarctic ozone will return to the 1980 level in the second half of the 21st century, in 2050–2070 period (Siddaway et al., 2013; Dameris and Godin-Beekmann, 2014, Solomon et al., 2016). Thus, slow ozone recovery will possibly continue about 3 times longer (~2000 to ~2060) than fast ozone depletion (1980–2000). If ozone depletion acts to significantly influence atmospheric asymmetries, slow reverse shifts of either or both the TOC minimum and QSW3 pattern could be expected in the future. However, due to possible influence of the greenhouse gas increase on the easward phase shift (Wang et al., 2013), after ozone recovery, the eastward shift in the QSW structure could be renewed.

As noted in Section 1, eastward shift in the QSW structure in the SH stratosphere can be attributed to changes in other aspects of the globally-coupled ocean–atmosphere system (Hio and Hirota, 2002; Malanca et al., 2005; Agosta and Canziani, 2011, Lin et al., 2010, 2012; Wang et al., 2013), including changing greenhouse gas concentration (Wang et al., 2013). Our work provides further evidence that asymmetries in the distribution of Antarctic spring ozone exhibit trends and variability that relate to both tropospheric processes and the action of ozone. Further investigation to separate the relative role of ozone depletion, climate change and natural climate variability on ozone asymmetries is required, and could be addressed using attribution experiments in climate models with both coupled oceans and interactive chemistry.

Author contribution

Based on ideas developed by G. P. M., A. V. G. performed data development and provided analysis with contribution from G. P. M., A. R. K. and O. M. E. G. P. M., A. R. K. and O. M. E. provided additional explanation of the outputs. A. V. G. prepared the manuscript with contributions from G. P. M., A. R. K. and O. M. E.

Acknowledgments. TOMS and OMI daily total ozone data provided by the Ozone Processing Team, NASA Goddard Space Flight Center, USA, from their Web site at http://ozoneaq.gsfc.nasa.gov. Multi-sensor reanalysis data from http://www.temis.nl are used. Data on ozone mass deficit in the Southern high latitudes are from http://ozonewatch.gsfc.nasa.gov. NCEP Reanalysis data provided by the NOAA/OAR/ESRL PSD, Boulder, Colorado, USA, from their Web site at http://www.esrl.noaa.gov/psd/. The ERA-Interim data from the European Centre

for Medium-Range Weather Forecasts reanalysis at http://www.ecmwf.int/en/research/climate-reanalysis/era-interim were used. This work was partly supported by Taras Shevchenko National University of Kyiv, project 16BF051-02, and by the Polar FORCeS project no. 4012 of the Australian Antarctic Science Program.

References

Agosta, E. A. and Canziani, P. O.: Interannual variations in the zonal asymmetry of the subpolar latitudes total ozone column during the austral spring, GeoActa, 35, 1–16. 2010.

Agosta, E. A. and Canziani, P. O.: Austral spring stratospheric and tropospheric circulation interannual variability, J. Climate, 24, 2629–2647, doi:10.1175/2010JCLI3418.1, 2011.

Albers, J. R. and Nathan, T. N.: Pathways for communicating the effects of stratospheric ozone to the polar vortex: Role of zonally asymmetric ozone, J. Atmos. Sci., 69, 785–801, doi:10.1175/JAS-D-11-0126.1, 2012.

Arblaster, J. M., Gillett, N. P. (Lead Authors), Calvo, N., Forster, P. M., Polvani, L. M., Son, S.-W., Waugh, D. W., and Young, P.J.: Stratospheric ozone changes and climate, Chapter 4 in Scientific Assessment of Ozone Depletion: 2014, Global Ozone Research and Monitoring Project – Report No. 55, World Meteorological Organization, Geneva, Switzerland, 2014.

Brasseur, G. P., Tie, X. X., Rasch, Ph. J., and Lefèvre, F.: A three-dimensional simulation of the Antarctic ozone hole: Impact of anthropogenic chlorine on the lower stratosphere and upper troposphere, J. Geophys. Res., 102, 8909–8930, doi:10.1029/96JD03398, 1997.

Chubachi, S. and Kajiwara, R.: Total ozone variations at Syowa, Antarctica, Geophys. Res. Lett., 13, 1197–1198, doi:10.1029/GL013i012p01197, 1986.

Crook, J. A., Gillett, N. P., and Keeley, S. P. E.: Sensitivity of Southern Hemisphere climate to zonal asymmetry in ozone, Geophys. Res. Lett., 35, L07806, doi:10.1029/2007GL032698, 2008.

Dameris, M., and Godin-Beekmann, S. (Lead Authors), Alexander, S., Braesicke, P., Chipperfield, M., de Laat, A. T. J., Orsolini, Y., Rex, M., and Santee, M. L.: Update on polar ozone: Past, present, and future, Chapter 3 in Scientific Assessment of Ozone Depletion: 2014, Global Ozone Research and Monitoring Project – Report No. 55, World Meteorological Organization, Geneva, Switzerland, 2014.

Dee, D. P., Uppala, S. M., Simmons, A. J., Berrisford, P., Poli, P., Kobayashi, S., Andrae, U., Balmaseda, M. A., Balsamo, G., Bauer, P., Bechtold, P., Beljaars, A., van de Berg, L., Bidlot, J., Bormann, N., Delsol, C., Dragani, R., Fuentes, M., Geer, A. J., Haimberger, L., Healy, S. B., Hersbach, H., Hólm, E. V., Isaksen, L., Kallberg, P., Köhler, M., Matricardi, M., McNally, A. P., Monge-Sanz, B. M., Morcrette, J.-J., Park, B. K., Peubey, C., de Rosnay, P., Tavolato, C., Thépaut, J.-N., and Vitart, F.: The ERA-Interim reanalysis: configuration and performance of the data assimilation system, Q. J. Roy. Meteorol. Soc., 137, 553–597, doi:10.1002/qj.828, 2011.

England, M. H., McGregor, S., Spence, P., Meehl, G.A., Timmermann, A., Cai, W., Sen Gupta, A., McPhaden, M. J., Purich, A. and Santoso, A. Recent intensification of wind-driven circulation

in the Pacific and the ongoing warming hiatus. Nature Climate Change, 4, 222-227, doi:10.1038/nclimate2106, 2014.

Farman, J. C., Gardiner, B. G., and Shanklin, J. D.: Large losses of total ozone in Antarctica reveal seasonal ClOx/NOx interaction, Nature, 315, 207–210, doi:10.1038/315207a0, 1985.

Fogt, R. L., Jones, J. M., and Renwick, J.: Seasonal zonal asymmetries in the Southern Annular Mode and their impact on regional temperature anomalies, J. Climate, 25, 6253–6270, doi:10.1175/JCLI-D-11-00474.1, 2012a.

Fogt, R. L., Wovrosh, A. J., Langen, R. A., and Simmonds, I.: The characteristic variability and connection to the underlying synoptic activity of the Amundsen-Bellingshausen Seas Low, J. Geophys. Res., 117, D07111, doi:10.1029/2011JD017337, 2012b.

Fogt, R. L., Perlwitz, J., Monaghan, A. J., Bromwich, D. H., Jones, J. M., and Marshall, G. J.: Historical SAM variability. Part II: Twentieth-century variability and trends from reconstructions, observations, and the IPCC AR4 models, J. Climate, 22, doi:10.1175/2009JCLI2786.1, 5346–5365, 2009.

Gabriel, A., Körnich, H., Lossow, S., Peters, D. H. W., Urban, J., and Murtagh, D.: Zonal asymmetries in middle atmospheric ozone and water vapour derived from Odin satellite data 2001–2010, Atmos. Chem. Phys., 11, 9865–9885, doi:10.5194/acp-11-9865-2011, 2011.

Gabriel, A., Peters, D., Kirchner, I., and Graf, H.-F.: Effect of zonally asymmetric ozone on stratospheric temperature and planetary wave propagation, Geophys. Res. Lett., 34, L06807, doi:10.1029/2006GL028998, 2007.

Gillett, N. P., Scinocca, J. F., Plummer, D. A., and Reader, M. C.: Sensitivity of climate to dynamically consistent zonal asymmetries in ozone, Geophys. Res. Lett., 36, L10809, doi:10.1029/2009GL037246, 2009.

Grassi, B., Redaelli, G., and Visconti, G.: Tropical SST preconditioning of the SH polar vortex during winter 2002, J. Climate, 21, 5295–5303, doi: 10.1175/2008JCLI2136.1, 2008.

Grytsai, A.: Planetary wave peculiarities in Antarctic ozone distribution during 1979–2008, Int. J. Remote Sens., 32, 3139–3152, doi:10.1080/01431161.2010.541518, 2011.

Grytsai, A., Grytsai, Z., Evtushevsky, A., and Milinevsky, G.: Interannual variability of planetary waves in the ozone layer at 65° S, Int. J. Remote Sens., 26, 3377–3387, doi:10.1080/01431160500076350, 2005.

Grytsai, A. V., Evtushevsky, O. M., Agapitov, O. V., Klekociuk, A. R., and Milinevsky, G. P.: Structure and long-term change in the zonal asymmetry in Antarctic total ozone during spring, Ann. Geophys., 25, 361–374, doi:10.5194/angeo-25-361-2007, 2007a.

Grytsai, A., Evtushevsky, A., Milinevsky, G., and Agapitov, A.: Longitudinal position of the quasi-stationary wave extremes over the Antarctic region from the TOMS total ozone, Int. J. Remote Sens., 28, 1391–1396, doi:10.1080/01431160600768021, 2007b.

Grytsai, A. V., Evtushevsky, O. M., and Milinevsky, G. P.: Anomalous quasi-stationary planetary waves over the Antarctic region in 1988 and 2002, Ann. Geophys., 26, 1101–1108, doi:10.5194/angeo-26-1101-2008, 2008.

Hartmann, D. L., Mechoso, C. R., and Yamazaki, K.: Observations of wave-mean flow interaction in the Southern Hemisphere, J. Atmos. Sci., 41, 351–362, doi:http://dx.doi.org/10.1175/1520-0469(1984)041<0351:OOWMFI>2.0.CO;2, 1984.

Hassler, B., Bodeker, G. E., Solomon, S., and Young, P. J.: Changes in the polar vortex: Effects on Antarctic total ozone observations at various stations, Geophys. Res. Lett., 38, L01805, doi:10.1029/2010GL045542, 2011.

Hio, Y. and Hirota, I. Interannual variations of planetary waves in the Southern Hemisphere stratosphere. J. Meteorol. Soc. Jap., 80, 1013–1027, 2002.

Hio, Y. and Yoden, S.: Quasi-periodic variations of the polar vortex in the Southern Hemisphere due to wave-wave interaction, J. Atmos. Sci., 61, 2510–2527, doi:http://dx.doi.org/10.1175/JAS3257.1, 2004.

Hirota, I. and Hirooka, T.: Normal mode Rossby waves observed in the upper stratosphere. Part I: First symmetric modes of zonal wavenumbers 1 and 2, J. Atmos. Sci., 41, 1253–1267, doi:http://dx.doi.org/10.1175/1520-0469(1984)041<1253:NMRWOI>2.0.CO;2. 1984.

Huth, R. and Canziani, P. O.: Classification of hemispheric monthly mean stratospheric potential vorticity fields, Ann. Geophys., 21, 805–817, doi:10.5194/angeo-21-805-2003, 2003.

Ialongo, I., Sofieva, V., Kalakoski, N., Tamminen, J., and Kyrölä, E.: Ozone zonal asymmetry and planetary wave characterization during Antarctic spring, Atmos. Chem. Phys., 12, 2603–2614, doi:10.5194/acp-12-2603-2012, 2012.

Kalnay, E., Kanamitsu, M., Kistler, R., Collins, W., Deaven, D., Gandin, L., Iredell, M., Saha, S., White, G., Woollen, J., Zhu, Y., Chelliah, M., Ebisuzaki, W., Higgins, W., Janowiak, J., Mo, K. C., Ropelewski, C., Wang, J., Leetmaa, A., Reynolds, R., Jenne, R., and Joseph, D.: The NCEP/NCAR 40-year Reanalysis Project, Bull. Amer. Meteorol. Soc., 77, 1057–1072, doi:http://dx.doi.org/10.1175/1520-0477(1996)077<0437:TNYRP>2.0.CO;2, 1996.

Krishnan, V.: Probability and random processes, John Wiley & Sons, Inc., Hoboken, New Jersey, 420 p., 2006.

Kuttippurath, J., Lefèvre, F., Pommereau, J.-P., Roscoe, H. K., Goutail, F., Pazmiño, A., and Shanklin, J. D.: Antarctic ozone loss in 1979–2010: first sign of ozone recovery, Atmos. Chem. Phys., 13, 1625–1635, doi:10.5194/acp-13-1625-2013, 2013.

Li, X., Holland, D. M., Gerber, E. P., and Yoo, C.: Impacts of the north and tropical Atlantic Ocean on the Antarctic Peninsula and sea ice, Nature, 505, 538–542, doi:10.1038/nature12945, 2014.

Lin, P., Fu, Q., Solomon, S., and Wallace, J. M.: Temperature trend patterns in Southern Hemisphere high latitudes: Novel indicators of stratospheric change, J. Climate, 23, 4264–4280, doi:10.1175/2009JCLI2971.1, 2010.

Lin, P, Fu, Q, and Hartmann, D. L.: Impact of tropical SST on stratospheric planetary waves in the Southern Hemisphere, J. Climate, 25. 5030–5046, doi:10.1175/JCLI-D-11-00378.1, 2012.

Malanca, F. E., Canziani, P. O., and Argüello, G. A.: Trends evolution of ozone between 1980 and 2000 at midlatitudes over the Southern Hemisphere: Decadal differences in trends, J. Geophys. Res., 110, D05102, doi:10.1029/2004JD004977, 2005.

Marshall, G. J.: Trends in the Southern Annular Mode from observations and reanalyses, J. Climate, 16, 4134–4143, doi:http://dx.doi.org/10.1175/1520-0442(2003)016<4134:TITSAM>2.0.CO;2, 2003.

Mo, K. C. and Higgins, R. W.: The Pacific-South American modes and tropical convection during the Southern Hemisphere winter, Mon. Wea. Rev., 126, 1581–1596, doi:http://dx.doi.org/10.1175/1520-0493(1998)126<1581:TPSAMA>2.0.CO;2, 1998.

Newman, P. A. and Nash, E. R.: The unusual Southern Hemisphere stratosphere winter of 2002, J. Atmos. Sci., 62, doi: http://dx.doi.org/10.1175/JAS-3323.1, 614–628, 2005.

Nishii, K. and Nakamura, H.: Tropospheric influence on the diminished Antarctic ozone hole in September 2002, Geophys. Res. Lett., 31, doi:10.1029/2004GL019532, 2004.

Peters, D. and Vargin, P.: Influence of subtropical Rossby wave trains on planetary wave activity over Antarctica in September 2002, Tellus, 67A, 25875, http://dx.doi.org/10.3402/tellusa.v67.25875, 2015.

Peters, D., Vargin, P., and Körnich, H.: A study of the zonally asymmetric tropospheric forcing of the austral vortex splitting during September 2002, Tellus, 59A, 384–394, doi: 10.1111/j.1600-0870.2007.00228.x, 2007.

Quintanar, A. I. and Mechoso, C. R.: Quasi-stationary waves in the Southern Hemisphere. Part I: Observational data, J. Climate, 8, 2659–2672, doi:http://dx.doi.org/10.1175/1520-0442(1995)008<2659:QSWITS>2.0.CO;2, 1995.

Randel, W. J.: The seasonal evolution of planetary waves in the southern hemisphere stratosphere and troposphere, Q. J. Roy. Meteorolog. Soc., 114, 1385–1409, doi:10.1002/qj.49711448403, 1988.

Raphael, M. N.: A zonal wave 3 index for the Southern Hemisphere, Geophys. Res. Lett., 31, L23212, doi:10.1029/2004GL020365, 2004.

Raphael, M. N., Marshall, G. J., Turner, J., Fogt, R. L., Schneider, D., Dixon, D. A., Hosking, J. S., Jones, J. M., and Hobbs, W. R.: The Amundsen Sea Low: Variability, change, and impact on Antarctic climate, Bull. Amer. Meteorol, Soc., 97, 111–121, doi:10.1175/BAMS-D-14-00018.1, 2016.

Roscoe, H. K., Feng, W., Chipperfield, M. P., Trainic, M., and Shuckburgh, E. F.: The existence of the edge region of the Antarctic stratospheric vortex, J. Geophys. Res., 117, D04301, doi:10.1029/2011JD015940, 2012.

Salby, M., Titova, E., and Deschamps, L.: Rebound of Antarctic ozone, Geophys. Res. Lett., 38, L09702, doi:10.1029/2011GL047266, 2011.

Schneider, D. P., Deser, C., and Fan, T.: Comparing the impacts of tropical SST variability and polar stratospheric ozone loss on the Southern Ocean westerly winds, J. Climate, 28, 9350 – 9372, doi:10.1175/JCLI-D-15-0090.1, 2015.

Siddaway, J. M., Petelina, S. V., Karoly, D. J., Klekociuk, A. R., and Dargaville, R. J.: Evolution of Antarctic ozone in September–December predicted by CCMVal-2 model simulations for the 21st century, Atmos. Chem. Phys., 13, 4413–4427, doi:10.5194/acp-13-4413-2013, 2013.

Solomon, S., Ivy D. J., Kinnison, D., Mills, M. J., Neely III, R. R., and Schmidt, A.: Emergence of healing in the Antarctic ozone layer, Science, 353(6296), 269-274, doi:10.1126/science.aae0061, 2016.

Solomon, S.: Stratospheric ozone depletion: a review of concepts and history, Rev. Geophys., 37, 275–316, doi:10.1029/1999RG900008, 1999.

Solomon, S., Portmann, R. W., Sasaki, T., Hofmann, D. J., and Thompson, D. W. J.: Four decades of ozonesonde measurements over Antarctica, J. Geophys. Res., 110, D21311, doi:10.1029/2005JD005917, 2005.

Son, S.-W., Purich, A., Hendon, H. H., Kim, B.-M., and Polvani, L. M.: Improved seasonal forecast using ozone hole variability?, Geophys. Res. Lett., 40, 6231–6235, doi:10.1002/2013GL057731, 2013.

Thompson, D. W. J., Solomon, S., Kushner, P. J., England, M. H., Grise, K. M., and Karoly, D. J.: Signatures of the Antarctic ozone hole in Southern Hemisphere surface climate change, Nature Geoscience, 4, 741–749, doi:10.1038/NGEO1296, 2011.

Thompson, D. W. J and Wallace, J.: Annular modes in the extratropical circulation. Part I: Month-to-month variability, J. Climate, 13, 1000–1016, doi:http://dx.doi.org/10.1175/1520-0442(2000)013<1000:AMITEC>2.0.CO;2, 2000.

Turner, J., Phillips, T., Hosking, J. S., Marshall, G. J., and Orr, A.: The Amundsen Sea low, Int. J. Climatol., 33, 1818–1829, doi:10.1002/joc.3558, 2013.

van der A, R. J., Allaart, M. A. F., Eskes, H. J.: Multi sensor reanalysis of total ozone, Atmos. Chem. Phys., 10, 11277–11294, doi:10.5194/acp-10-11277-2010, 2010.

Varotsos, C. A., Milinevsky, G., Grytsai, A., Efstathiou, M., and Tzanis, C.: Scaling effect in planetary waves over Antarctica, Int. J. Remote Sens., 29, 2697–2704, doi:10.1080/01431160701767559, 2008.

Wang, L., Kushner, P. J. and Waugh, D. W.: Southern Hemisphere stationary wave response to changes of ozone and greenhouse gases, J. Climate, 26, 10205–10217, doiI:http://dx.doi.org/10.1175/JCLI-D-13-00160.1, 2013.

Waugh, D. W., Oman, L., Newman, P. A., Stolarski, R. S., Pawson, S., Nielsen, J. E., and Perlwitz, J.: Effect of zonal asymmetries in stratospheric ozone on simulated Southern Hemisphere climate trends, Geophys. Res. Lett., 36, L18701, doi:10.1029/2009GL040419, 2009.

Waugh, D. W. and Randel, W.J.: Climatology of Arctic and Antarctic polar vortices using elliptical diagnostics, J. Atmos. Sci., 56, 1594–1613, doi:http://dx.doi.org/10.1175/1520-0469(1999)056<1594:COAAAP>2.0.CO;2, 1999.

Wirth, V.: Quasi-stationary planetary waves in total ozone and their correlation with lower stratospheric temperature, J. Geophys. Res., 98, 8873–8882, doi:10.1029/92JD02820, 1993.

Atmos. Chem. Phys. Discuss., doi:10.5194/acp-2016-537, 2016
Manuscript under review for journal Atmos. Chem. Phys.
Published: 4 August 2016

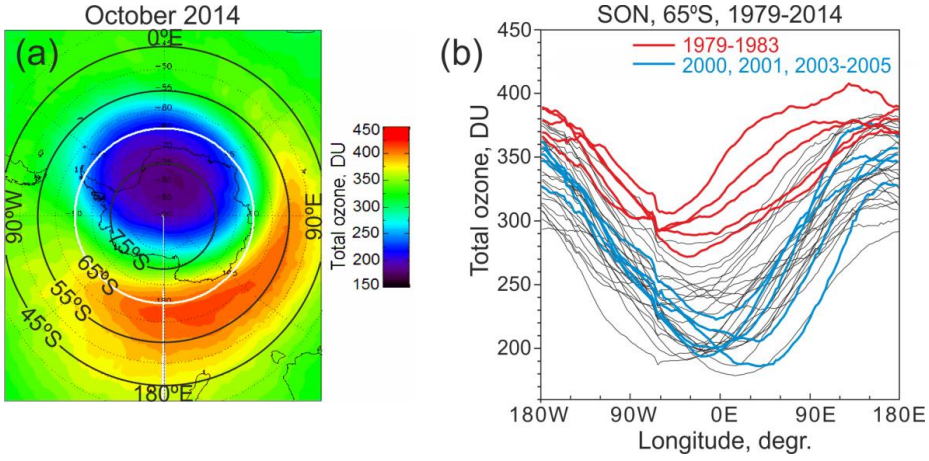

Figure 1: (a) Total ozone in the SH middle/high latitudes in October 2014. (b) Zonal dependence of the total ozone at 65°S averaged for September–November for each year between 1979 and 2014; Red curves show pre-ozone hole years 1979–1983 and blue curves show the years of maximum ozone hole 2000–2005 (with the exception of the anomalous 2002). Modified from Grytsai et al. (2007a).

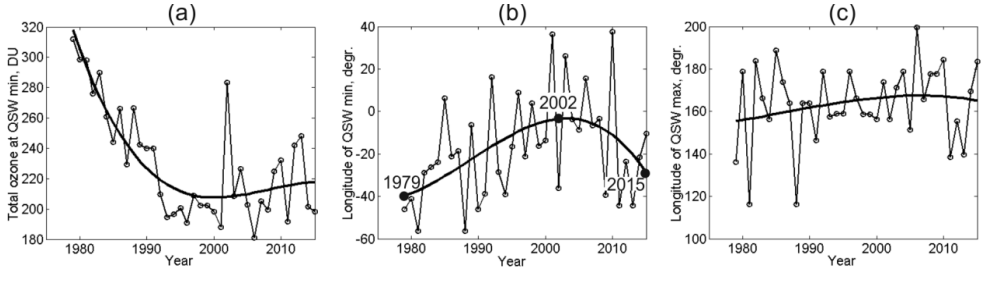

Figure 2: (a) Total ozone at zonal QSW minimum, (b) longitude of QSW minimum and (c) longitude of the QSW maximum at 65°S averaged for September–November. Thin lines are timeseries of 1979–2015 and thick lines are polynomial fits of degree 3. Longitudes for 1979, 2002 and 2015 from polynomial fitting are marked in (b) by closed circles.

Atmos. Chem. Phys. Discuss., doi:10.5194/acp-2016-537, 2016
Manuscript under review for journal Atmos. Chem. Phys.
Published: 4 August 2016

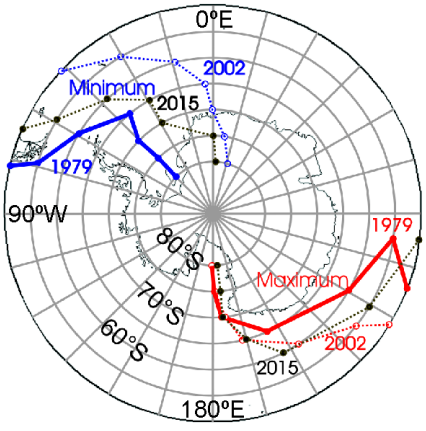

Figure 3: Map of longitudinal locations of zonal QSW maximum (red) and zonal QSW minimum (blue) at seven latitudes between 50°S and 80°S; westernmost (easternmost) longitudes in 1979 (2002) determined from the polynomial fit, as shown in Fig. 2b, are connected with thick (thin) lines. Black dotted line marks longitudes for 2015. Modified from Grytsai et al. (2007a).

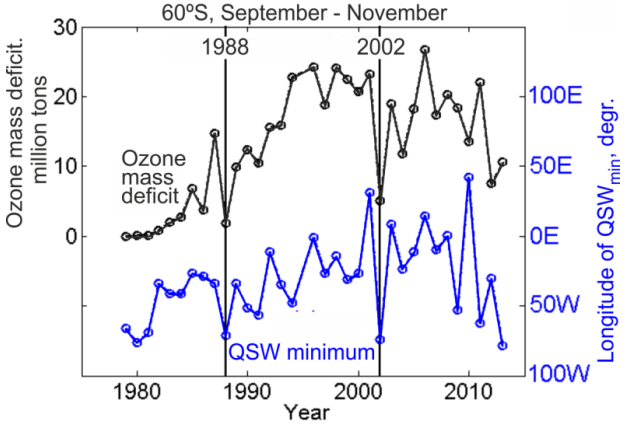

Figure 4: Ozone mass deficit and position of the quasi-stationary minimum in the ozone distribution at 60°S averaged over September–November. Pearson correlation coefficient between the two timeseries is r = 0.57. Data for the ozone mass deficit in the SH high latitudes are from http://ozonewatch.gsfc.nasa.gov/meteorology/SH.html. Years of large (1988) and extreme (2002) stratospheric warmings are indicated by vertical lines.

Atmos. Chem. Phys. Discuss., doi:10.5194/acp-2016-537, 2016
Manuscript under review for journal Atmos. Chem. Phys.
Published: 4 August 2016

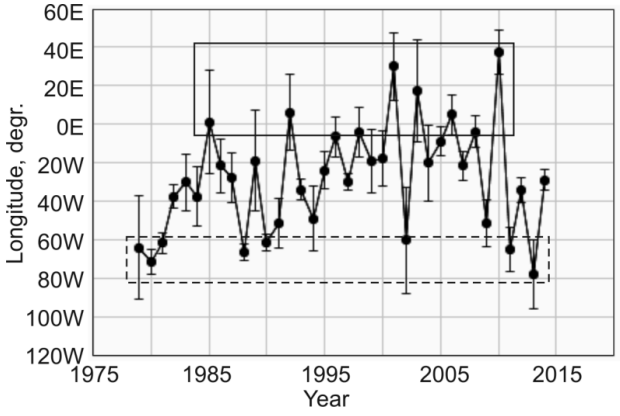

Figure 5: Longitude of MSR TOC ozone minimum (QSW_{min}) for SON averaged over four latitudes between 55° S and 70° S, inclusive. The vertical bars span ±1 standard deviation of the individual values used in each average. The solid (dashed) rectangle outlines the upper 80th percentile (lower 20th percentile) corresponding to the maximal eastward (westward) shift of the QSW_{min} longitude.

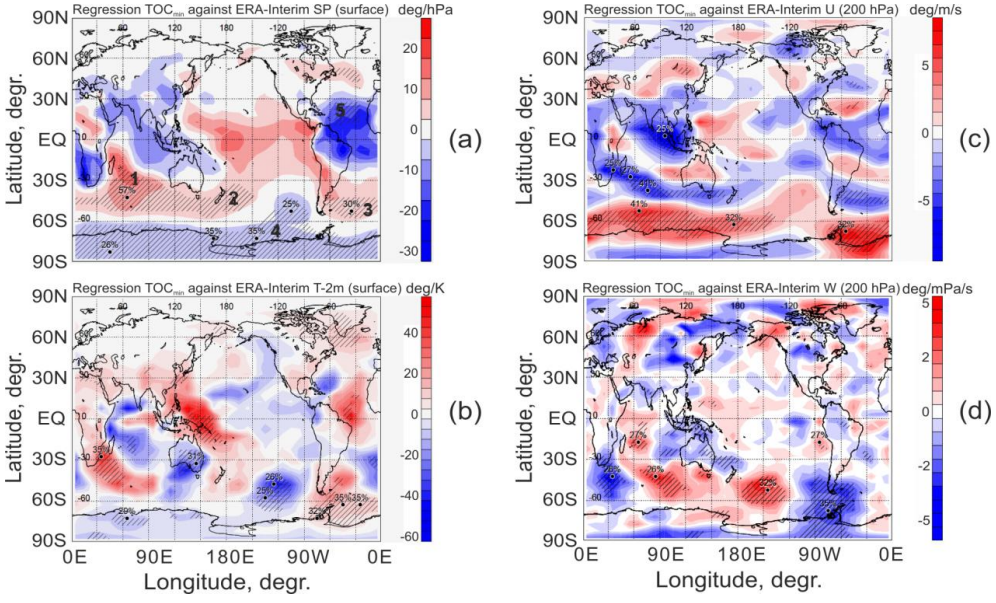

Figure 6: Regression coefficient of the TOC QSW minimum longitude against ERA-Interim climatological anomalies of (a) surface pressure (SP), (b) 2 metre air temperature (T-2m), (c) 200-hPa zonal wind speed (U200) and (d) 200-hPa vertical pressure wind speed (W200) for SON 1979–2014. The units are degrees of longitude per: (a) hPa, (b) K, (c) m s^{-1} and (d) mPa s^{-1}. The hatching is shown where the correlation between the two variables in each panel is significant at the 95% confidence limit.

Atmos. Chem. Phys. Discuss., doi:10.5194/acp-2016-537, 2016
Manuscript under review for journal Atmos. Chem. Phys.
Published: 4 August 2016

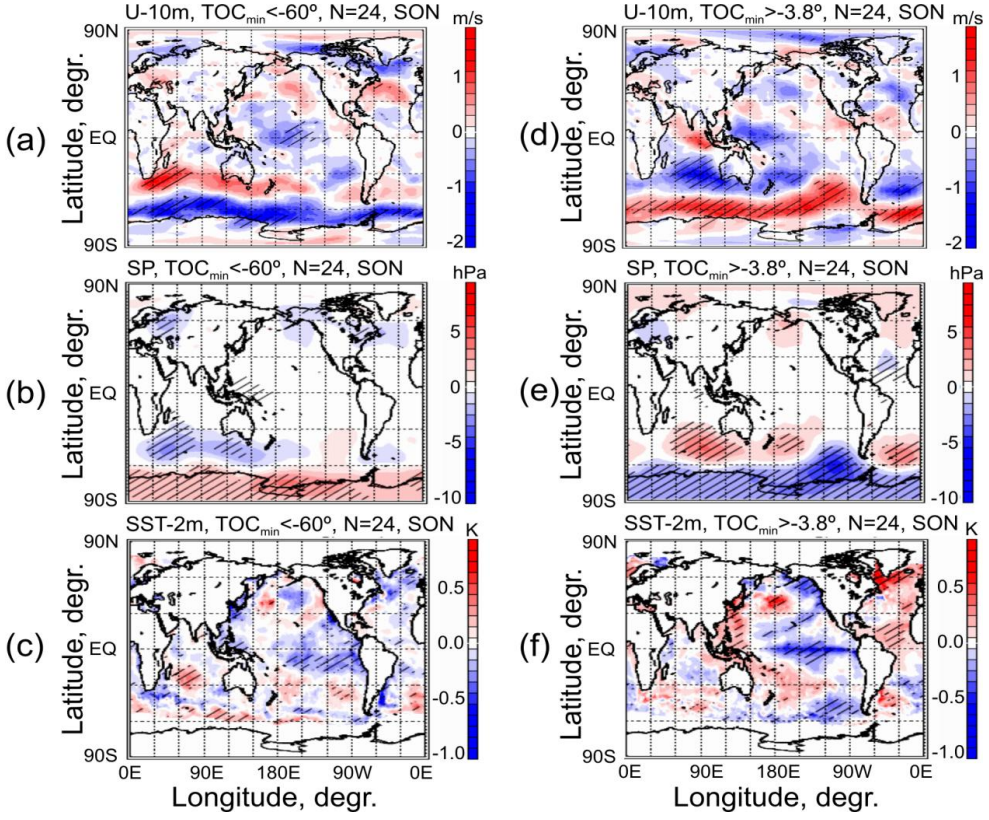

Figure 7: Anomaly composites with respect to the mean climatology for 1979-2014 of ERA-Interim surface meteorological variables for (left) the lower 20th percentile of mean SON QSW$_{min}$ longitudes (western phases) and (right) the upper 80th percentile of mean SON QSW$_{min}$ longitudes (eastern phases). Rows (from top to bottom) are (a, d) 10-m zonal wind (U-10m in m s^{-1}), (b, e) surface pressure (SP in hPa) and (c, f) sea surface temperature (SST in K). Diagonal shading indicates regions significant at the 95% confidence limit (evaluated by comparing the value of each grid box with its standard deviation).

Atmos. Chem. Phys. Discuss., doi:10.5194/acp-2016-537, 2016
Manuscript under review for journal Atmos. Chem. Phys.
Published: 4 August 2016

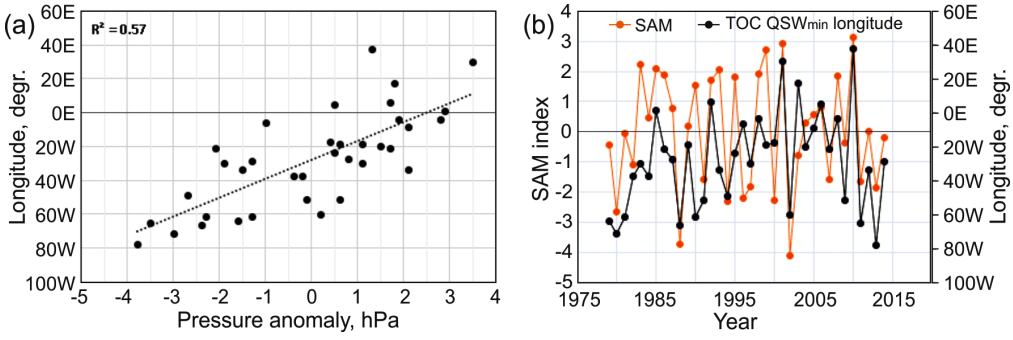

Figure 8: (a) Regression of surface pressure anomaly for grid box 1 (42.5°S, 65.0°E) of Fig. 6a (horizontal axis) against the QSW_{min} longitude (vertical axis). (b) Timeseries of the standardized SAM index (orange, left axis) and the QSW_{min} longitude (black, right axis). The timeseries of the QSW_{min} longitude is that shown in Fig. 5. All variables are averaged over September–November. The R^2 value is significant at the 95% confidence limit.

Atmos. Chem. Phys. Discuss., doi:10.5194/acp-2016-537, 2016
Manuscript under review for journal Atmos. Chem. Phys.
Published: 4 August 2016

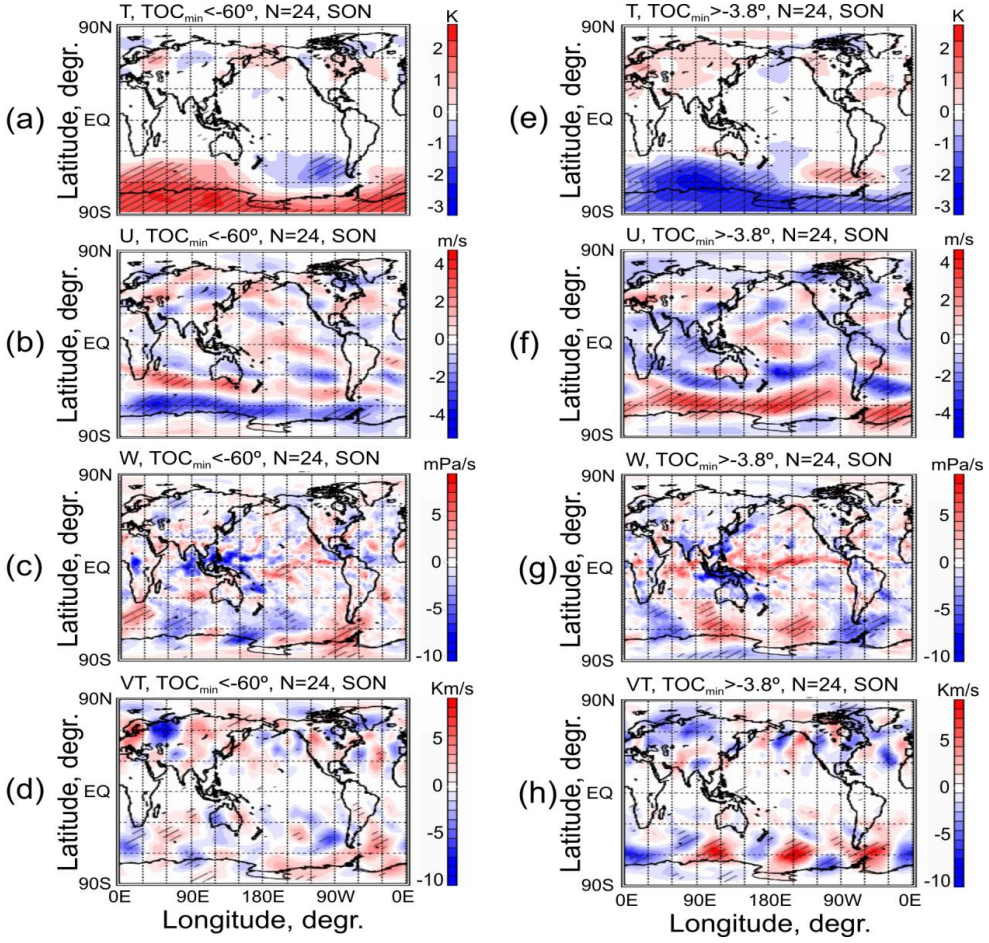

Figure 9: As in Fig. 7, but for ERA-Interim meteorological variables at 200 hPa: (a, e) air temperature (T200 in K), (b, f) zonal wind (U200 in m s^{-1}), (c, g) vertical pressure wind (W200 in mPa s^{-1}), and (d, h) eddy heat flux ($V'T'$ in K m s^{-1}). Diagonal shading indicates as in Figure 7.

Atmos. Chem. Phys. Discuss., doi:10.5194/acp-2016-537, 2016
Manuscript under review for journal Atmos. Chem. Phys.
Published: 4 August 2016

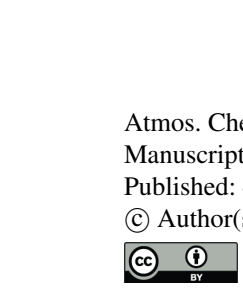

Atmospheric Chemistry and Physics Discussions

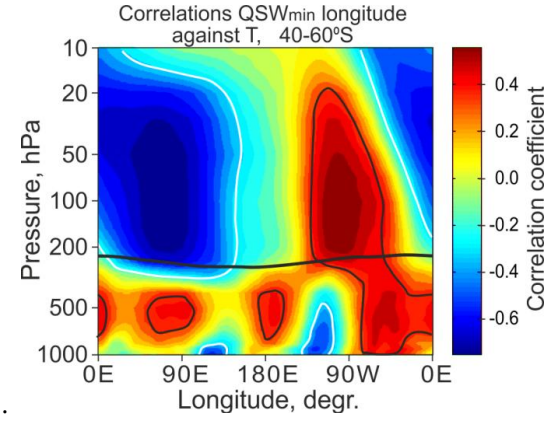

Figure 10: Longitude–height cross-section of the correlation between the QSW_{min} longitude at 65°S and air temperature averaged over the zone 40–60°S for SON 1979–2014. Thick black curve marks climatological thermal tropopause from the NCEP–NCAR reanalysis. Black (white) contours show positive (negative) correlations significant at the 95% confidence limit.

775

Atmos. Chem. Phys. Discuss., doi:10.5194/acp-2016-537, 2016
Manuscript under review for journal Atmos. Chem. Phys.
Published: 4 August 2016

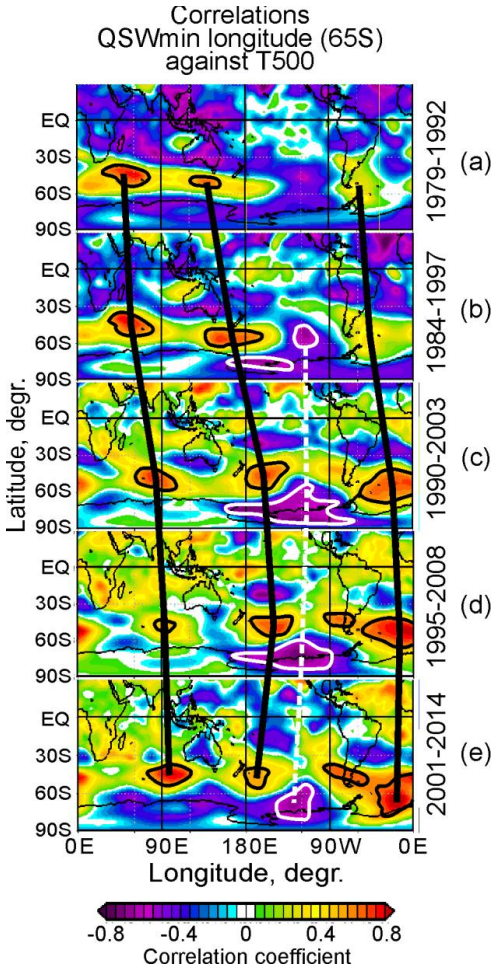

Figure 11: Correlation between the QSW_{min} longitude at 65°S and air temperature at 500 hPa south of 30°N. Five sequential 14-year intervals with 5-6-year step are presented. Black (white) contours show positive (negative) correlations significant at the 95% confidence limit. Thick solid black (dashed white) lines mark mean longitudinal positions of the positive (negative) correlation peaks in the QSW3 structure.